BEC BIOENERGETICS COMMUNICATIONS
Bioenerg Commun 2022.14.
https://doi.org/10.26124/bec:2022-0014
Open Access

Experimental Communication

Cite
Ganguly U, Bir A, Chakrabarti S (2022) Cytotoxicity of mitochondrial Complex I inhibitor rotenone: a complex interplay of cell death pathways. Bioenerg Commun 2022.14. https://doi.org/10.26124/bec:2022-0014

Author contributions
All authors performed data collection and evaluation and cowrote the manuscript.

Conflicts of interest
The authors declare they have no conflict of interest.

Received 2022-04-14
Reviewed 2022-07-19
Revised 2022-08-08
Accepted 2022-11-19
Published 2022-11-22

Open peer review
TuuliKaambre (editor)
Timea Komlodi (reviewer)
Nicoleta Moisoi (reviewer)
Marcus Oliveira (reviewer)

Data availability
Data are not available in open repository but may be obtained from the corresponding author.

Keywords
rotenone Rot;
mitochondria mt;
ferroptosis;
reactive oxygen and nitrogen species RONS;
neurodegeneration

Cytotoxicity of mitochondrial Complex I inhibitor rotenone: a complex interplay of cell death pathways

Upasana Ganguly[1], Aritri Bir[2], Sasanka Chakrabarti[1*]

[1] Dept Biochem Central Res Lab, Maharishi Markandeshwar Inst Med Sci Res, Maharishi Markandeshwar University (Deemed to be), Mullana, Ambala, India
[2] Dept Biochem, Dr BC Roy Multispeciality Med Res Centre, IIT Kharagpur, India

* Corresponding author: profschakrabarti95@gmail.com

Summary

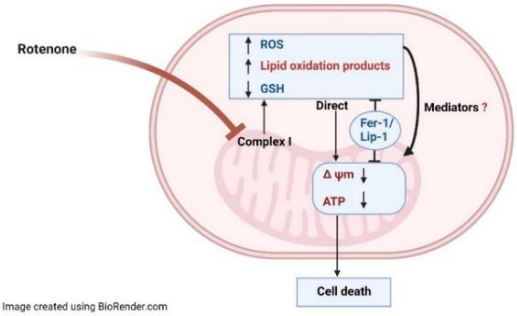

Ferroptosis, a type of regulated cell death, has been implicated in various diseases like cancer and neurodegenerative diseases including Parkinson's disease. Because the mitochondrial Complex I inhibitor rotenone is widely used to develop experimental models of Parkinson's disease, we examined if rotenone is an inducer of ferroptosis. Ferroptosis is iron-dependent and accompanied by increased production and accumulation of reactive oxygen and nitrogen species and lipid oxidation products, depletion of reduced glutathione, mitochondrial morphological alterations, and rupture of the plasma membrane. The mechanism of cell death in ferroptosis subsequent to the accumulation of ROS and lipid oxidation products, however, is not clearly established. We show here that rotenone (0.5 µM) causes the death of SH-SY5Y cells (a human neuroblastoma cell line) within 48 h accompanied by mitochondrial membrane depolarization, intracellular ATP depletion, increased production and accumulation of ROS and the lipid oxidation product malondialdehyde and a decrease in reduced

glutathione content. These processes are inhibited conspicuously by novel inhibitors of ferroptosis such as ferrostatin-1 and liproxstatin-1 without rescuing the rotenone-induced inhibition of Complex I activity. Further, after rotenone-treatment both apoptotic and necrotic cells were noticed as evidenced from nuclear morphology after staining by Hoechst 33258 and propidium iodide, respectively. Taken together, rotenone was an inducer of ferroptosis in SH-SY5Y cells which presented morphological features of apoptosis and necrosis.

1. Introduction

An important sub-type of regulated cell death called ferroptosis has been under intensive investigation over the last few years, and the process is implicated in diseases including cancer and neurodegenerative diseases (Li et al 2020; Jiang et al 2021). Ferroptosis is an iron-dependent pathway of regulated cell death accompanied by an excess production and accumulation of reactive oxygen and nitrogen species (RONS), lipid-derived oxyradicals, and various lipid peroxidation products. In a broad sense RONS include not only the classical reactive oxygen species like the superoxide radical, H_2O_2 and hydroxyl radicals, but also the lipid hydroperoxides, lipid- and protein-derived oxyradicals, peroxynitrite radicals and others (Stockwell et al 2017; Cheng et al 2018). Along with the enhanced production and accumulation of RONS, a depletion of glutathione, mitochondrial morphological alterations, and the rupture of the cell membrane occur; the process is inhibited by iron-chelators, e.g. deferoxamine and lipophilic antioxidants such as vitamin E, butylated hydroxytoluene, ferrostatin-1 (Fer-1) and liproxstatin-1 (Lip-1) (Xie et al 2016; Stockwell et al 2017). Ferroptotic cell death apparently depends on accumulation of lipid peroxidation intermediates and products, and thus novel lipophilic antioxidants Fer-1 and Lip-1 are particularly effective in preventing ferroptosis (Zilka et al 2017). Ferroptosis can be triggered by many different pharmacological agents, which cause a depletion or decreased synthesis of major intracellular antioxidants such as reduced glutathione (GSH), inhibit the antioxidant enzyme glutathione peroxidase 4 (Gpx4), or cause an increase in the intracellular iron content (Jiang et al 2021; Li et al 2020). Several pathways regulating or initiating ferroptosis in cells have been identified primarily by genetic studies, but definite mechanisms or mediators executing cell death following the accumulation of ROS and lipid oxidation products are yet to be established in ferroptosis. Because ferroptosis is an iron-dependent process and mitochondria are the most important sources of ROS generation *in vivo*, it is important to investigate how mitochondrial bioenergetic alterations are involved in ferroptotic cell death. In fact, mitochondrial respiratory inhibitors and TCA cycle intermediates have been implicated in complex and contradictory ways with ferroptosis (Gao et al 2019; Yao et al 2021; Gan 2021).

Linking ferroptosis with neuronal death in neurodegenerative diseases such as Alzheimer's disease (AD) or Parkinson's disease (PD) is an attractive proposition because both increased iron accumulation and oxidative damage in specific brain regions are key pathological features of these diseases (Ganguly et al 2017). Unlike AD, several toxins-based animal models are quite popular in analyzing PD pathogenesis or screening for

potential anti-parkinsonian drugs (Duty, Jenner 2011; Betarbet et al 2002). Despite the limitations of cell-based models to mimic the pathologic scenario of a complex disease such as PD, the cytotoxic mechanisms of several PD-related toxins such as 1-methyl-4-phenyl-1,2,3,6-tetrahydropyridine (MPTP), 6-hydroxydopamine, and rotenone have been extensively studied in different cell lines and primary cultures of neurons (Ke et al 2021). Rotenone, a classical inhibitor of Complex I, causes cell death, redox imbalance, and impaired mitochondrial bioenergetics in experimental models, but the mechanisms of cytotoxicity of rotenone are not fully elucidated and various mechanisms of cell death are reported (Barrientos, Moraes 1999; Moon et al 2005; Radad et al 2006; Xiong et al 2013; Callizot et al 2019). For example, from an elaborate study where Complex I inhibition was induced by genetic manipulation or rotenone treatment, it was concluded that rotenone-induced cell death could be ascribed to increased oxidative stress instead of a simple ATP depletion as a result of Complex I inhibition (Barrientos, Moraes 1999). Likewise, rotenone-induced death in SK-N-MC (human neuroblastoma cell line) cells was prevented by α-tocopherol. Under this condition increased oxidative stress was suggested as the mechanism of neural cell death as a result of Complex I inhibition (Sherer et al 2003). On the other hand, another study distinguished two different mechanisms of rotenone-induced death in dopaminergic and non-dopaminergic neuronal cells. Thus, in non-dopaminergic MN9X cells, rotenone caused cell death mediated by oxidative damage, while rotenone-mediated death of dopaminergic MN9D cells was attributed to mitochondrial bioenergetic disruption by Complex I inhibition (Kweonet al 2004). Similarly, rotenone at low concentrations caused the death of primary ventral mesencephalic neurons of rats by Complex I inhibition and associated mitochondrial membrane depolarization, which was not prevented by several antioxidants (Moon et al 2005).

Thus, the exact pathway of rotenone-induced cell death remains unclear. It may partly depend on the concentration of rotenone and the nature of the cell line used. This may explain why apoptosis, autophagy, and necrosis have been suggested (Barrientos, Moraes 1999; Callizot et al 2019; Xiong et al 2013; Radad et al 2006). Multiple links between rotenone cytotoxicity, ferroptosis and intracellular iron dyshomeostasis have been indicated in some studies. Thus, rotenone-induced ROS production, morphological changes, α-synuclein aggregation, and activation of apoptosis in SH-SY5Y cells could be prevented by ferrostatin-1 which is a typical antioxidant trapping lipid-derived oxyradicals and inhibiting ferroptosis (Kabiraj et al 2015). Likewise, another interesting study reported that rotenone exposure of SH-SY5Y cells increased the levels of transferrin receptor 1 and divalent metal transporter 1 but decreased the cellular level of ferroportin 1; these changes led to an increase in iron uptake with an increase in the intracellular labile pool of iron and consequent oxidative stress (Urrutia et al 2017). This study further showed that the knockdown of iron-responsive element binding protein 1 (IRP-1) prevents rotenone-induced iron dyshomeostasis, oxidative stress, and cell death (Urrutia et al 2017).

Over this backdrop and given the fact that mitochondrial dysfunction and ferroptotic death are possibly interlinked in the pathogenesis of Parkinson's disease, we were prompted to re-examine the rotenone-induced death of SH-SY5Y cells with a focus on ferroptosis and mitochondria. SH-SY5Y cells were selected for this study because this catecholaminergic human neuroblastoma cell line is widely used to investigate the mechanisms of PD neurodegeneration (Xicoy et al 2017).

2. Materials and methods

2.1. Cell culture and treatment protocol

SH-SY5Y cells undifferentiated (NCCS, Pune, India) were maintained in a medium composed of 2 volumes of Dulbecco's modified Eagle's medium (DMEM; ThermoFisher, USA) and 1 volume of Ham's F12 medium containing 10 % fetal bovine serum (ThermoFisher, USA); penicillin 50 units/mL, streptomycin 50 µg/mL (Penicillin-Streptomycin; ThermoFisher, USA), and amphotericin B (2.5 µg/mL; Sigma, USA). The final medium also contained 20 mM glucose and 3 mM glutamine. For experimental purposes, the cells were grown and manipulated in plastic tissue culture flasks, multi-well tissue culture plates, or poly- L-lysine coated coverslips under a humidified atmosphere of 5 % CO_2 and 95 % air at 37 °C. The cells were treated without (control) or with rotenone (0.5 µM; Sigma, USA) for 48 h in the presence or absence of ferrostatin-1 (Fer-1, 1 µM; Sigma, USA), liproxstatin-1 (Lip-1, 1 µM; Sigma, USA), or other additions followed by the analysis of various biochemical and microscopic parameters.

2.2. Measurement of cell viability

The cell viability was assessed by the Trypan blue assay and LDH release assay (Ganguly et al 2020). In the Trypan blue assay, the dead (blue-stained) and live cells were counted by an automated cell counter (ThermoFisher Scientific, USA), which was cross-verified by manual counting by two observers each counting 250 – 300 cells. In addition, the LDH released into the medium in each well was assayed spectrophotometrically by monitoring the oxidation of NADH (SRL, India) at 340 nm using pyruvate as the substrate; the activity of the enzyme released in each well was normalized by protein content and expressed as a percentage of LDH released in reference wells with 100 % cell death (cells treated for 48 h with 10 µM antimycin A; Sigma, USA) (Ganguly et al 2020).

2.3. Measurements of oxidative stress parameters

RONS production and cellular levels of malondialdehyde (MDA) and reduced glutathione were measured as oxidative stress parameters in controls and experimental groups of treated SH-SY5Y cells. For RONS measurement, the fluorogenic ROS probe, 2', 7'-dichlorodihydrofluorescein diacetate H_2DCFDA (Sigma, USA), was utilized; intracellular esterases hydrolyzed H_2DCFDA to release $DCFH_2$, which reacted with RONS to produce a fluorescent product (λ_{ex} 485 nm, λ_{em} 535 nm) (Jana et al 2011). The assay was conducted with the cells in 96-well plates; after removal of the medium, each well was gently rinsed twice with phosphate-buffered saline, pH 7.4 (PBS), removing dead cells and debris. The adherent cells were incubated with a serum-free medium containing 10 µM H_2DCFDA at 37 °C for 30 min in the dark, followed by removal of the medium and two washings with PBS. The cells in each well were finally covered with 200 µL PBS, and the fluorescence intensity was measured in a multi-mode plate reader (Molecular Devices, USA). Importantly, H_2DCFDA is not a specific probe for any particular RONS, but interacts with H_2O_2, hydroxyl radicals, lipid hydroperoxides, peroxynitrite, and peroxyl radicals; in a broad sense as indicated already, RONS encompasses all these radicals, and several others (Gomes et al 2005; Kalyanaraman et al 2012; Cheng et al 2018). However, the reaction chemistry of H_2DCFDA assay is complex and it can be affected by several intracellular components such as cytochrome *c*, heme, and transition metals (Dikalov, Harrison 2014).

The cellular content of GSH was determined by the 5,5´-dithio-bis-nitrobenzene (DTNB; Sigma, USA) assay. After brief washings in PBS, the cells were re-suspended in 100 mM potassium phosphate buffer / 5 mM EDTA, pH 7.5 (KPE buffer), extracted by brief vortexing with an equal volume of 0.1 % Triton X-100 in 5 % trichloroacetic acid in KPE buffer and centrifuged at 4 °C at 10000 *g* for 5 min. The supernatant was used to measure GSH by allowing it to react with DTNB in KPE buffer at 37 °C for 10 min, and the color developed was read at 412 nm. The method was adapted from Rahman et al (2006) and Look et al (1997).

Measurement of MDA was based on the 2-thiobarbituric acid (TBA; HiMedia, India) assay according to Draper et al (1993).

2.4. Measurement of mitochondrial parameters

The mitochondrial membrane potential and ATP content of control and treated SH-SY5Y cells were measured by tetramethylrhodamine ethyl ester TMRE (Sigma, USA) and luciferin-luciferase-based assays, respectively according to Ganguly et al (2020) and Singh et al (2022). Briefly, the control and treated cells were maintained on 96 well plates for 48 h, and after the incubation, the medium from each well was removed followed by two gentle washings with 200 µL of phosphate-buffered saline (PBS) to remove the dead cells and the debris, and the adherent cells were analyzed for mitochondrial membrane potential or cellular ATP content.

In the TMRE assay, the adherent cells were further incubated in serum-free medium with 100 nM TMRE for 15 min at 37 °C. At the end of the incubation, the medium was removed, the attached cells were delicately washed with PBS twice, and then covered with 100 µL PBS. Finally, the fluorescence intensity was recorded at λ_{ex} 549 nm and λ_{em} 575 nm in a multi-mode plate reader (Molecular Devices, USA). The values were expressed as percentages of the control after normalization for protein content of the corresponding wells. In each set of TMRE assays, carbonyl cyanide 4-(trifluoromethoxy) phenylhydrazone (FCCP; Sigma, USA)-treated cells were analyzed as positive controls for membrane depolarization.

For the ATP assay, the adherent cells (control and treated) were lysed with an ice-cold hypotonic buffer containing 10 mM Tris, 1 mM EDTA, 0.5 % Triton X-100, pH 7.6. The cell lysate was mixed immediately with the ATP assay mix as per the manufacturer's protocol (Sigma, USA) and the chemiluminescence readings from different wells were recorded using a multi-mode microplate reader (Molecular Devices, USA). A calibration curve of ATP (0.08 – 40 nM) was used to calculate the actual concentration of ATP in the cell lysate.

For the Complex I-III (NADH-cytochrome *c* reductase activity) assay, mitochondria were isolated from the cells as described earlier (Jana et al 2011). The Complex I-III assay was performed spectrophotometrically using NADH as the electron donor and ferricytochrome *c* (Sigma, USA) as the electron acceptor. The reaction was monitored by following the rate of reduction of ferricytochrome *c* at 540 nm (Bagh et al 2011).

2.5. Nuclear staining by Hoechst and propidium iodide

Hoechst 33258 dye (Invitrogen, USA) was used for the identification of apoptotic nuclei (Jana et al 2011). SH-SY5Y cells were grown on poly-L-lysine coated coverslips and treated without (control) or with rotenone (0.5 µM) for 48 h. The cells were washed twice

with PBS, fixed with 4 % paraformaldehyde for 10 min, and re-washed twice with PBS. The fixed cells were then incubated with 1 µg/mL Hoechst 33258 dye for 20 min at 37 °C. After staining, the coverslips were rinsed with PBS, mounted on glass slides, and observed under a fluorescence microscope (Carl Zeiss, Germany). For PI staining, control and treated cells grown on 24-well plates were suspended by trypsinization, centrifuged, and the pelleted cells were fixed with 70 % ethanol for 10 min. The cells were then washed twice with PBS and re-suspended in PBS with propidium iodide PI (1 µM; ThermoFisher, USA) for 20 min at 37 °C. The stained cells were collected by centrifugation, washed with PBS twice to remove the excess dye, and observed under a fluorescence microscope (Carl Zeiss, Germany).

2.6. Protein determination

Protein was determined by the bicinchoninic acid (BCA; Sigma, USA) assay (Smith et al 1985). The samples were solubilized in 1 % sodium dodecyl sulfate (SDS) before estimation of protein.

2.7. Statistical analysis

Statistical significance among three or more groups was performed by one-way analysis of variance (ANOVA) followed by Tukey's posthoc test after checking for the normality of data distribution. Graphpad Prism version 8.4.2 was used for statistical calculations. A p-value of ≤ 0.05 was considered statistically significant; actual p values of all comparisons were indicated in the figure legends and highly significant differences between the groups were shown as $p < 0.0001$ as obtained from the software output chart. Values are represented as the medians with range and scatterplots reflecting the individual data points.

3. Results

Results presented in Figure 1 show that rotenone (0.5 µM) caused a marked loss of cell viability after 48 h of incubation; a comparable and more than a 5.5-fold increase of cell death with respect to control cells was observed both in Trypan blue and LDH release assays. Cell death was prevented to a large extent when the cells were co-incubated with Fer-1 (1 µM) or Lip-1 (1 µM) along with rotenone (Figure 1).

When SH-SY5Y cells were incubated with rotenone (0.5 µM) for 48 h, a nearly 4.5-fold increase in the level of MDA — an end product of lipid peroxidation — was observed compared to that in control cells which was abolished nearly completely by co-treatment with Fer-1 and Lip-1. The generation of RONS in rotenone-treated SH-SY5Y cells increased about 4.5-fold over the control value which was prevented markedly by Fer-1 or Lip-1 (Figure 2). The major cellular antioxidant GSH was depleted noticeably upon rotenone-treatment of SH-SY5Y cells for 48 h which was largely rescued by co-treatment with Fer-1 and Lip-1 (Figure 2).

Three important parameters related to mitochondrial functions were affected by the rotenone-treatment of SH-SY5Y cells for 48 h as presented in Figure 3. Mitochondrial transmembrane potential and cellular ATP content were decreased by nearly 60 % when SH-SY5Y cells were incubated for 48 h with 0.5 µM rotenone, and these effects were markedly, but not completely, prevented by co-treatment of the cells with Fer-1 and Lip-1

(Figure 3). Complex I-III (NADH-cytochrome *c* reductase) activity was inhibited by about 50 % after the rotenone-treatment of SH-SY5Y cells for 48 h, but Fer-1 or Lip-1 did not show protection against rotenone (Figure 3).

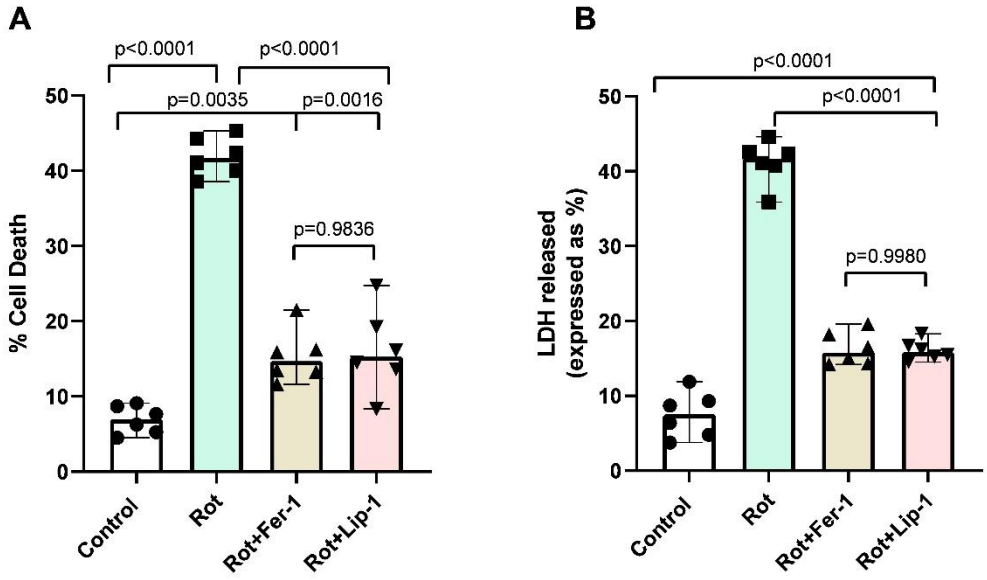

Figure 1. Ferrostatin-1 and Liproxstatin-1 prevent rotenone-induced cell death. SH-SY5Y cells were treated without (Control) or with Rotenone (Rot, 0.5 μM) in the presence or absence of ferrostatin-1 (Fer-1, 1 μM) or liproxstatin-1 (Lip-1, 1 μM) for 48 h. Cell viability was analyzed by **(A)** Trypan blue assay and **(B)** LDH release assay. Values are medians and range of six observations (independent) shown as scatterplots of individual data points.

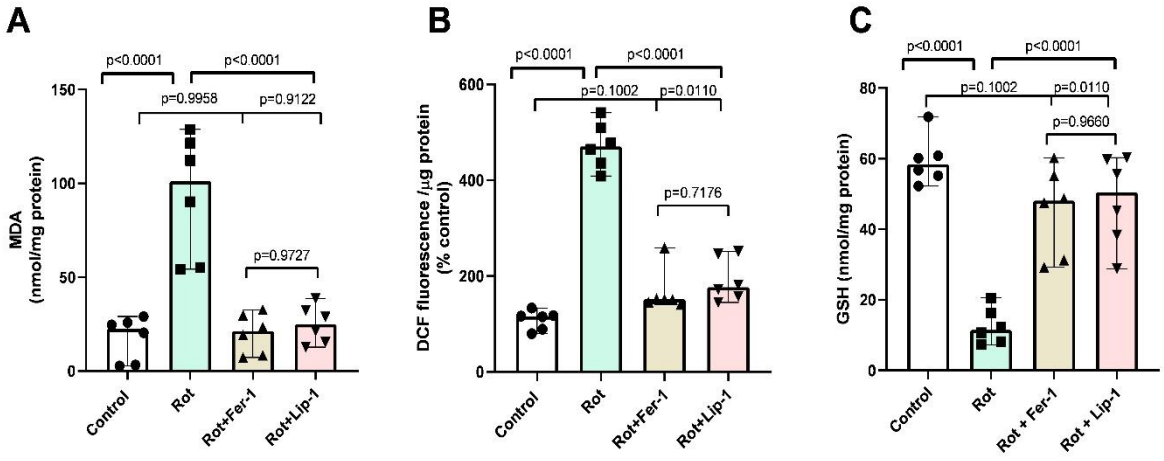

Figure 2. Rotenone-mediated oxidative stress in SH-SY5Y cells. SH-SY5Y cells were treated without (Control) or with Rotenone (Rot, 0.5 μM) in the presence or absence of ferrostatin-1 (Fer-1, 1 μM) or liproxstatin-1 (Lip-1, 1 μM). After 48h of incubation, the cells were analyzed for MDA **(A)**, RONS **(B)**, and GSH **(C)** content. Values are represented as medians and range of six independent experiments.

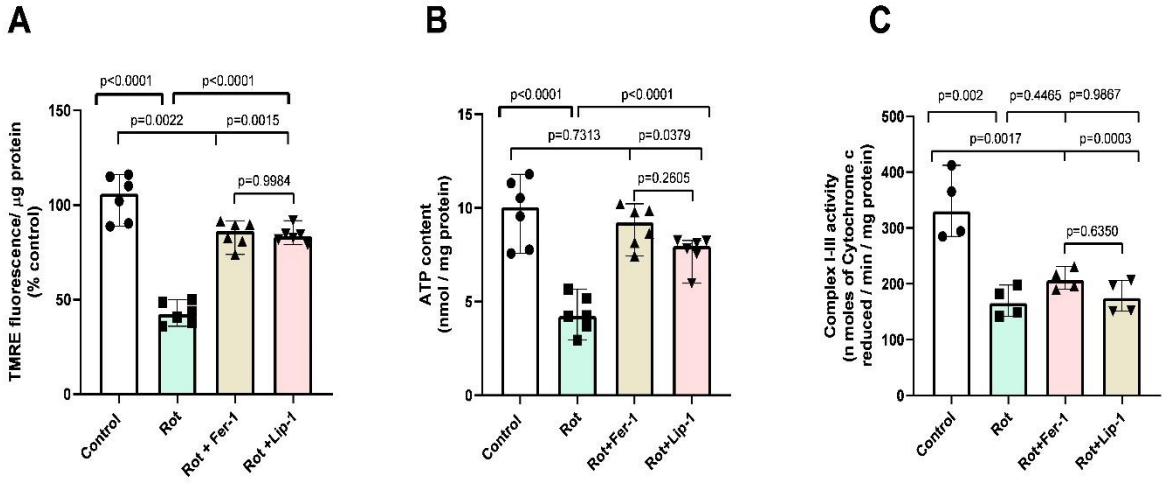

Figure 3. Effects of Ferrostatin-1 and Liproxstatin-1 on rotenone-mediated mitochondrial dysfunction. SH-SY5Y cells were either untreated (Control) or treated with Rotenone (Rot, 0.5 µM) with or without ferrostatin-1 (Fer-1, 1 µM) or liproxstatin-1 (Lip-1, 1 µM) for 48 h. The cells were analyzed for **(A)** mitochondrial membrane potential using the TMRE assay, **(B)** intracellular ATP content, or **(C)** mitochondrial Complex I-III activity. The experiments were performed in six biological replicates for (A) and (B) and four biological replicates for (C). Values are represented as medians and range indicating individual data points in scatterplots.

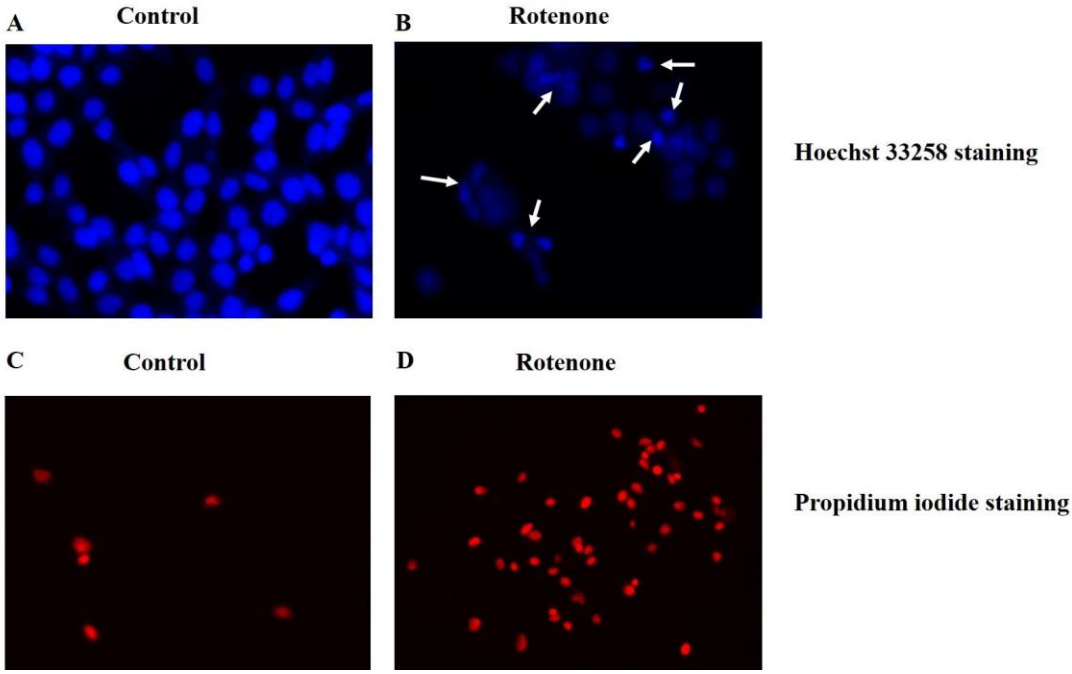

Figure 4. Nuclear staining Hoechst 33258 and PI. SH-SY5Y cells were treated without (Control) or with Rotenone (0.5 µM) for 48 h. The cells were stained by Hoechst 33258 **(A & B)** or PI **(C & D)**. A representative image from a set of 4 independent experiments. The white arrows indicate the apoptotic nuclei (**B**).

When SH-SY5Y cells were treated with rotenone (0.5 μM) for 48 h and the cells were examined under a fluorescence microscope after staining with Hoechst 33258, many brightly fluorescent and condensed nuclei were noticed indicating apoptotic cells; likewise, an examination of PI-stained cells after similar rotenone-treatment revealed many bright red fluorescent nuclei indicative of plasma membrane rupture and necrosis (Figure 4).

4. Discussion

Inhibition of Complex I (measured as NADH-ubiquinone reductase) and NADH-cytochrome *c* reductase were initially observed in the substantia nigra of postmortem PD brains, and subsequently, other mitochondrial anomalies were reported in this disease from postmortem studies (Schapira et al 1990; Toulorge et al 2016). At the experimental level, Complex I inhibitors such as MPTP and rotenone are widely used toxins to develop animal models of PD (Duty, Jenner 2011; Richardson et al 2007). However, the mechanisms of rotenone cytotoxicity are not definitively established, as indicated at the beginning of this article. Though several studies suggest that a simple bioenergetic failure of the cell after Complex I inhibition by rotenone triggers cell death, other studies demonstrated the predominant role of oxidative stress in this process (Barrientos, Moraes 1999; Sherer et al 2003; Li et al 2003; Kweon et al 2004; Moon et al 2005). In an elegant study with dopaminergic neurons obtained from Ndufs4 (a gene necessary for Complex I assembly)-deficient mice, it was shown that rotenone toxicity was not prevented in cells deficient in Complex I activity implying other mechanisms and targets of rotenone toxicity (Choi et al 2008). It is quite possible that increased production of ROS with associated oxidative stress could be the pivotal mechanism of cytotoxicity in rotenone-treated cells given the known involvement of ROS in differently regulated cell death pathways. The enhanced formation of ROS could be the result of Complex I inhibition by rotenone, but other mechanisms may also be involved such as the increased intracellular labile pool of iron as a result of altered expression levels of iron-transport proteins in rotenone-treated cells (Urrutia et al 2017).

Our current study demonstrated that rotenone could induce cell death and an increased accumulation of ROS and lipid peroxidation end products, and depletion of GSH, which were prevented markedly by the inhibitors of ferroptosis Fer-1 and Lip-1; these observations indicate rotenone-induced ferroptosis under our experimental conditions. Although mitochondrial morphological changes have been characteristically described in ferroptosis, the precise involvement of mitochondria in ferroptosis has remained controversial in many respects (Gao et al 2019; Gan 2021; Wang et al 2020). For example, mitochondrial membrane hyperpolarization was reported by classical inducers of ferroptosis such as erastin (Gao et al 2019). On the other hand, t-butyl hydroperoxide was shown to trigger ferroptosis in PC12 cells with mitochondrial membrane depolarization and loss of ATP, and our results are consistent with this study (Wu et al 2018). In melanoma cells, the Complex I inhibitor BAY 87-2243 causes ferroptosis and necroptosis with mitochondrial membrane depolarization (Basit et al 2017). Our results further show that Fer-1 and Lip-1 rescued the rotenone-induced loss of mitochondrial membrane potential and cellular ATP content, but not inhibition of Complex I, implying that the latter phenomenon *per se* was not responsible for mitochondrial bioenergetic impairment. Instead, the accumulation of ROS and lipid peroxidation products in rotenone-treated cells was responsible for mitochondrial dysfunction and cell death. Our results are,

therefore, in conformity with those studies that suggested oxidative stress instead of a bioenergetic failure from direct Complex I inhibition as the key mechanism of rotenone toxicity (Barrientos, Moraes 1999; Sherer et al 2003; Li et al 2003). This oxidative stress-mediated cell death upon rotenone exposure is further supported by a study that showed activation of the oxidative stress-sensitive kinases p38 and c-Jun N-terminal protein kinase (JNK) in SH-SY5Y cells after rotenone treatment which was linked to apoptotic cell death (Newhouse et al 2004). In a recently published study related to the rotenone toxicity in SH-SY5Y cells, we reported that mitochondrial membrane depolarization, decreased cellular ATP content, increased ROS production, and cell death at 48 h of rotenone exposure were markedly prevented by cyclosporine A, implying that these effects were the result of activation of the mitochondrial permeability transition pore mtPTP (Singh et al 2022). In the same study, we further showed that cell death and ROS production in rotenone-treated cells during the early phase of exposure at 4 h or 24 h were much less compared to that at 48 h and were not noticeably preventable by cyclosporine A (Singh et al 2022). These results suggest that during rotenone exposure an initial increase of ROS production occurs presumably by Complex I inhibition resulting in some cell death, but gradually the build-up of ROS through free radical chain reactions activates the mtPTP leading to pronounced cell death, mitochondrial impairment, and further ROS production at the later phase. This scenario agrees well with the results of the current study; Fer-1 and Lip-1 prevented the build-up of RONS and oxidative stress during rotenone exposure and thereby blocked the subsequent mtPTP activation. Thus, Fer-1 and Lip-1 prevented mitochondrial impairment, cell death, and further ROS production observed at 48 h in the current study. It is not known at this juncture if ROS directly activates mtPTP, or other mediators are involved in this process. Interestingly in the current study, the Hoechst 33258 and PI staining of SH-SY5Y cells after rotenone treatment for 48 h indicated a mixed pattern of necrosis and apoptosis which was expected given the involvement of mtPTP in this process. The activation of mtPTP is mechanistically linked with both apoptosis and necrosis (Kinnally et al 2011; Redza-Dutordoir, Averill-Bates 2016). This mixed pattern of apoptosis and necrosis in rotenone-treated cells agrees with earlier reports by Radad et al (2006) and Hong et al (2014).

Though our study has demonstrated the central role of RONS and oxidative stress in rotenone cytotoxicity, it does not explain why in some other studies the direct bioenergetic failure, as from Complex I inhibition by rotenone, was the underlying mechanism of cell death (Moon et al 2005; Kweon et al 2004). It is possible that during the early phase or under lower doses of rotenone exposure or in specific cell types the alternative mechanism (Complex I-induced bioenergetic failure) is operative. It is necessary to delineate these two different mechanisms of cell death by carefully controlling the two mechanisms under different experimental conditions. Likewise, the nature of the cells (primary neurons dopaminergic or non-dopaminergic, differentiated or undifferentiated neural cell lines or non-neural cell lines) exert a significant influence on the mechanism of rotenone toxicity which should be explored thoroughly. It would be interesting to examine the effects of the ferroptosis inhibitors Fer-1 and Lip-1 on rotenone toxicity under different experimental conditions. However, in the current study where the oxidative mechanism of rotenone toxicity is operative, it is understandable why molecules like Fer-1, Lip-1, and cyclosporine A are capable of preventing cell death without recovering the Complex I activity (Singh et al 2022). It is tempting to speculate that under conditions of the oxidative mechanism of rotenone toxicity some metabolic re-programming compensates for the bioenergetic impairment of Complex I inhibition but

cannot rescue the cells from oxidative death. Thus, it would be interesting to explore this aspect of metabolic re-programming in rotenone-treated cells under two different mechanisms of cell death *vis-à-vis* the protective role of Fer-1, Lip-1, or cyclosporine A. Additionally, some studies indicate other toxic effects of rotenone at higher concentrations, such as the disorganization of microtubular structures linked with apoptosis (Barrientos, Moraes 1999).

In conclusion, our short report implicates rotenone as a ferroptotic inducer, and further implies the involvement of mitochondria in ferroptotic cell death. When analyzed in combination with another related recent publication of our group, it is evident that mtPTP activation is a key event of ferroptotic death which exhibits the features of both apoptosis and necrosis. Further, we have suggested from a literature survey and our results how rotenone toxicity could follow different mechanisms under different experimental conditions. At the translational level, the results are important because ferroptosis is now considered a possible mechanism of neurodegeneration in PD, and rotenone is widely used to develop experimental models of PD. The neuroprotective potential of Fer-1 or Lip-1 in animal models of PD should be explored further for a new therapeutic approach for PD.

Abbreviations

AD	Alzheimer's disease	PBS	phosphate-buffered saline
Fer-1	ferrostatin-1	PD	Parkinson's disease
GSH	reduced glutathione	ROS	reactive oxygen species
LDH	lactate dehydrogenase	RONS	reactive oxygen and nitrogen species
Lip-1	liproxstatin-1		
MDA	malondialdehyde	TCA	tricarboxylic acid
MPTP	1-methyl-4-phenyl-1,2,3,6-tetrahydropyridine	TMRE	tetramethylrhodamine ethyl ester
mtPTP	mitochondrial permeability transition pore		

Acknowledgements

SC acknowledges the financial support received from Indian Council of Medical Research (ICMR), Government of India [Sanction No. 5/4-5/191/Neuro/2019-NCD-I].

References

Bagh MB, Thakurta IG, Biswas M, Behera P, Chakrabarti S (2011) Age-related oxidative decline of mitochondrial functions in rat brain is prevented by long term oral antioxidant supplementation. https://doi.org/10.1007/s10522-010-9301-8

Barrientos A, Moraes CT (1999) Titrating the effects of mitochondrial complex I impairment in the cell physiology. https://doi.org/10.1074/jbc.274.23.16188

Basit F, van Oppen LM, Schöckel L, Bossenbroek HM, van Emst-de Vries SE, Hermeling JC, Grefte S, Kopitz C, Heroult M, Hgm Willems P, Koopman WJ (2017) Mitochondrial complex I inhibition triggers a mitophagy-dependent ROS increase leading to necroptosis and ferroptosis in melanoma cells. https://doi.org/10.1038/cddis.2017.133

Betarbet R, Sherer TB, Greenamyre JT (2002) Animal models of Parkinson's disease. https://doi.org/10.1002/bies.10067

Callizot N, Combes M, Henriques A, Poindron P (2019) Necrosis, apoptosis, necroptosis, three modes of action of dopaminergic neuron neurotoxins. https://doi.org/10.1371/journal.pone.0215277

Cheng G, Zielonka M, Dranka B, Kumar SN, Myers CR, Bennett B, Garces AM, Dias Duarte Machado LG, Thiebaut D, Ouari O, Hardy M, Zielonka J, Kalyanaraman B (2018) Detection of mitochondria-generated reactive oxygen species in cells using multiple probes and methods: potentials, pitfalls, and the future. https://doi.org/10.1074/jbc.RA118

Choi WS, Kruse SE, Palmiter RD, Xia Z (2008) Mitochondrial complex I inhibition is not required for dopaminergic neuron death induced by rotenone, MPP^+, or paraquat. https://doi.org/10.1073/pnas.0807581105

Dikalov SI, Harrison DG (2014) Methods for detection of mitochondrial and cellular reactive oxygen species. https://doi.org/10.1089/ars.2012.4886

Draper HH, Squires EJ, Mahmoodi H, Wu J, Agarwal S, Hadley M (1993) A comparative evaluation of thiobarbituric acid methods for the determination of malondialdehyde in biological materials. https://doi.org/10.1016/0891-5849(93)90035-s

Duty S, Jenner P (2011) Animal models of Parkinson's disease: a source of novel treatments and clues to the cause of the disease. https://doi.org/10.1111/j.1476-5381.2011.01426.x

Gan B (2021) Mitochondrial regulation of ferroptosis. https://doi.org/10.1083/jcb.202105043

Ganguly G, Chakrabarti S, Chatterjee U, Saso L (2017) Proteinopathy, oxidative stress and mitochondrial dysfunction: cross talk in Alzheimer's disease and Parkinson's disease. https://doi.org/10.2147/dddt.s130514

Ganguly U, Banerjee A, Chakrabarti SS, Kaur U, Sen O, Cappai R, Chakrabarti S (2020) Interaction of α-synuclein and Parkin in iron toxicity on SH-SY5Y cells: implications in the pathogenesis of Parkinson's disease. https://doi.org/10.1042/bcj20190676

Gao M, Yi J, Zhu J, Minikes AM, Monian P, Thompson CB, Jiang X (2019) Role of mitochondria in ferroptosis. https://doi.org/10.1016/j.molcel.2018.10.042

Gomes A, Fernandes E, Lima JL (2005) Fluorescence probes used for detection of reactive oxygen species. https://doi.org/10.1016/j.jbbm.2005.10.003

Hong Y, Nie H, Wu D, Wei X, Ding X, Ying Y (2014) NAD(+) treatment prevents rotenone-induced apoptosis and necrosis of differentiated PC12 cells. https://doi.org/10.1016/j.neulet.2013.11.039

Jana S, Sinha M, Chanda D, Roy T, Banerjee K, Munshi S, Patro BS, Chakrabarti S (2011) Mitochondrial dysfunction mediated by quinone oxidation products of dopamine: Implications in dopamine cytotoxicity and pathogenesis of Parkinson's disease. https://doi.org/10.1016/j.bbadis.2011.02.013

Jiang X, Stockwell BR, Conrad M (2021) Ferroptosis: mechanisms, biology and role in disease. https://doi.org/10.1038/s41580-020-00324-8

Kabiraj P, Valenzuela CA, Marin JE, Ramirez DA, Mendez L, Hwang MS, Varela-Ramirez A, Fenelon K, Narayan M, Skouta R (2015) The neuroprotective role of ferrostatin-1 under rotenone-induced oxidative stress in dopaminergic neuroblastoma cells. https://doi.org/10.1007/s10930-015-9629-7

Kalyanaraman B, Darley-Usmar V, Davies KJ, Dennery PA, Forman HJ, Grisham MB, Mann GE, Moore K, Roberts LJ 2nd, Ischiropoulos H (2012) Measuring reactive oxygen and nitrogen species with fluorescent probes: challenges and limitations. https://doi.org/10.1016/j.freeradbiomed.2011.09.030

Ke M, Chong CM, Zhu Q, Zhang K, Cai CZ, Lu JH, Qin D, Su H (2021) Comprehensive perspectives on experimental models for Parkinson's disease. https://doi.org/10.14336/ad.2020.0331

Kinnally KW, Peixoto PM, Ryu SY, Dejean LM (2011) Is mPTP the gatekeeper for necrosis, apoptosis, or both? https://doi.org/10.1016/j.bbamcr.2010.09.013

Kweon GR, Marks JD, Krencik R, Leung EH, Schumacker PT, Hyland K, Kang UJ (2004) Distinct mechanisms of neurodegeneration induced by chronic complex I inhibition in dopaminergic and non-dopaminergic cells. https://doi.org/10.1074/jbc.M407336200

Li J, Cao F, Yin HL, Huang ZJ, Lin ZT, Mao N, Sun B, Wang G (2020) Ferroptosis: past, present, and future. https://doi.org/10.1038/s41419-020-2298-2

Li N, Ragheb K, Lawler G, Sturgis J, Rajwa B, Melendez JA, Robinson JP (2003) Mitochondrial complex I inhibitor rotenone induces apoptosis through enhancing mitochondrial reactive oxygen species production. https://doi.org/10.1074/jbc.m210432200

Look MP, Rockstroh JK, Rao GS, Kreuzer KA, Barton S, Lemoch H, Sudhop T, Hoch J, Stockinger K, Spengler U, Sauerbruch T (1997) Serum selenium, plasma glutathione (GSH) and erythrocyte glutathione peroxidase (GSH-Px)-levels in asymptomatic versus symptomatic human immunodeficiency virus-1 (HIV-1)-infection. https://doi.org/10.1038/sj.ejcn.1600401

Moon Y, Lee KH, Park JH, Geum D, Kim K (2005) Mitochondrial membrane depolarization and the selective death of dopaminergic neurons by rotenone: protective effect of coenzyme Q_{10}. https://doi.org/10.1111/j.1471-4159.2005.03112.x

Newhouse K, Hsuan SL, Chang SH, Cai B, Wang Y, Xia Z (2004) Rotenone-induced apoptosis is mediated by p38 and JNK MAP kinases in human dopaminergic SH-SY5Y cells. https://doi.org/10.1093/toxsci/kfh089

Radad K, Rausch WD, Gille G (2006) Rotenone induces cell death in primary dopaminergic culture by increasing ROS production and inhibiting mitochondrial respiration. https://doi.org/10.1016/j.neuint.2006.02.003

Rahman I, Kode A, Biswas SK (2006) Assay for quantitative determination of glutathione and glutathione disulfide levels using enzymatic recycling method. https://doi.org/10.1038/nprot.2006.378

Redza-Dutordoir M, Averill-Bates DA (2016) Activation of apoptosis signalling pathways by reactive oxygen species. https://doi.org/10.1016/j.bbamcr.2016.09.012

Richardson JR, Caudle WM, Guillot TS, Watson JL, Nakamaru-Ogiso E, Seo BB, Sherer TB, Greenamyre JT, Yagi T, Matsuno-Yagi A, Miller GW (2007) Obligatory role for complex I inhibition in the dopaminergic neurotoxicity of 1-methyl-4-phenyl-1,2,3,6-tetrahydropyridine (MPTP). https://doi.org/10.1093/toxsci/kfl133

Schapira AHV, Cooper JM, Dexter D, Clark JB, Jenner P, Marsden CD (1990) Mitochondrial complex I deficiency in Parkinson's disease. https://doi.org/10.1111/j.1471-4159.1990.tb02325.x

Sherer TB, Betarbet R, Testa CM, Seo BB, Richardson JR, Kim JH, Miller GW, Yagi T, Matsuno-Yagi A, Greenamyre JT (2003) Mechanism of toxicity in rotenone models of Parkinson's disease. https://doi.org/10.1523/JNEUROSCI.23-34-10756.2003

Singh S, Ganguly U, Pal S, Chandan G, Thakur R, Saini RV, Chakrabarti SS, Agrawal BK, Chakrabarti S (2022) Protective effects of cyclosporine A on neurodegeneration and motor impairment in rotenone-induced experimental models of Parkinson's disease. https://doi.org/10.1016/j.ejphar.2022

Smith PK, Krohn RI, Hermanson GT, Mallia AK, Gartner FH, Provenzano MD, Fujimoto EK, Goeke NM, Olson BJ, Klenk DC (1985) Measurement of protein using bicinchoninic acid. https://doi.org/10.1016/0003-2697(85)90442-7

Stockwell BR, Angeli JPF, Bayir H, Bush AI, Conrad M (2017) Ferroptosis: A regulated cell death nexus linking metabolism, redox biology, and disease. https://doi.org/10.1016/j.cell.2017.09.021

Toulorge D, Schapira AHV, Hajj R (2016) Molecular changes in the postmortem Parkinsonian brain. https://doi.org/10.1111/jnc.13696

Urrutia PJ, Aguirre P, Tapia V, Carrasco CM, Mena NP, Núñez MT (2017) Cell death induced by mitochondrial complex I inhibition is mediated by Iron Regulatory Protein 1. https://doi.org/10.1016/j.bbadis.2017.05.015

Wang H, Liu C, Zhao Y, Gao G (2020) Mitochondria regulation in ferroptosis. https://doi.org/10.1016/j.ejcb.2019.151058

Wu C, Zhao W, Yu J, Li S, Lin L, Chen X (2018) Induction of ferroptosis and mitochondrial dysfunction by oxidative stress in PC12 cells. https://doi.org/10.1038/s41598-017-18935-1

Xicoy H, Wieringa B, Martens GJM (2017) The SH-SY5Y cell line in Parkinson's disease research: a systematic review. https://doi.org/10.1186/s13024-017-0149-0

Xie Y, Hou W, Song X, Yu Y, Huang J, Sun X, Kang R, Tang D (2016) Ferroptosis: process and function. https://doi.org/10.1038/cdd.2015.158

Xiong N, Xiong J, Jia M, Liu L, Zhang X, Chen Z, Huang J, Zhang Z, Hou L, Luo Z, Ghoorah D, Lin Z, Wang T (2013) The role of autophagy in Parkinson's disease: rotenone-based modeling. https://doi: 10.1186/1744-9081-9-13

Yao X, Li W, Fang D, Xiao C, Wu X, Li M, Luo Z (2021) Emerging roles of energy metabolism in ferroptosis regulation of tumor cells. https://doi.org/10.1002/advs.20210099

Zilka O, Shah R, Li B, FriedmannAngeli JP, Griesser M, Conrad M, Pratt DA (2017) On the mechanism of cytoprotection by ferrostatin-1 and liproxstatin-1 and the role of lipid peroxidation in ferroptotic cell death. https://doi.org/10.1021/acscentsci.7b00028